

EVALUATION OF FRAGILITY CURVES FOR A THREE-STOREY REINFORCED CONCRETE MOCK-UP OF SMART 2013 PROJECT

Luis A. Dalguer¹, Philippe Renault¹, Sergey Churilov² and Christoph Butenweg³

¹ swissnuclear, Aarauerstrasse 55, 4601 Olten, Switzerland (corresponding author: luis.dalguer@swissnuclear.ch)

² Ss.Cyril and Methodius University, Faculty of Civil Engineering, Blvd. Partizanski odredi 24, 1000 Skopje, Macedonia

³ SDA-engineering GmbH, Kaiserstr. 100, 52134 Herzogenrath, Germany

ABSTRACT

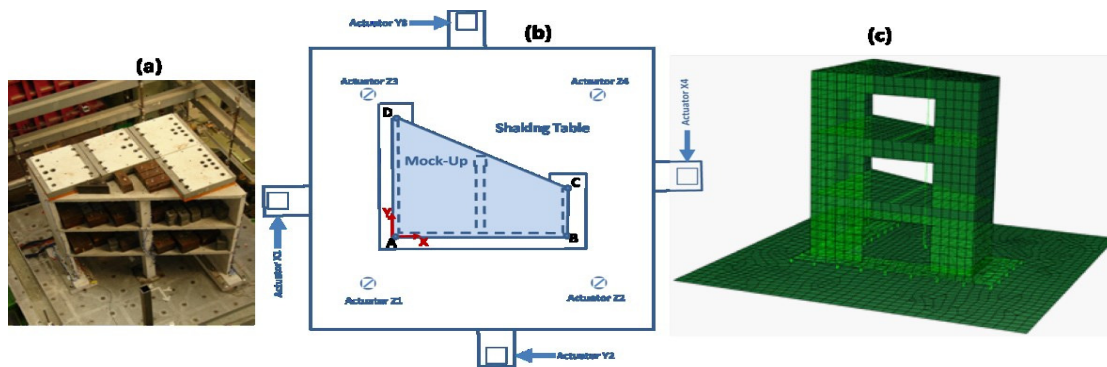
There is an increasing awareness of the need to use synthetic ground-motion time series in combination with observed data for the assessment of seismic vulnerability (risk) of critical structures such as nuclear power plants. In this paper synthetic ground motion data is used to evaluate the damage of an unsymmetric three-storey reinforced concrete (RC) mock-up tested within the framework of the SMART 2013 project (<http://www.smart2013.eu>). This building has been selected because of the availability of detailed structural and observed shaking data that provide a unique opportunity to study such a type of structures. The concrete damage plasticity model available in ABAQUS has been used as constitutive model. The nonlinear material imposes limits to the accelerations and displacements of the structural response around the first two fundamental frequencies of the structure, with amplitude reduction of about 50% in comparison to the linear response. The largest inter-story drift occurs during the shaking, and visible deviation from the linear response initiates at the beginning of the strong shaking. Fragility curves are calculated assuming maximum inter-story drift as damage indicator in two perpendicular directions. The probability of damage substantially differs between the two directions due to the unsymmetric geometrical features of the structure.

INTRODUCTION

Most of the locations of Nuclear Installations in Europe are in low seismicity area. The hazard in these zones predicts moderate to large events (e.g. Woessner et al., 2012) that are required for the input of risk assessment of critical structures such as nuclear power plants. But observed data for such events at the site of study are not currently available. Therefore, there is an increasing awareness of the need to use synthetic ground-motion time series in combination with observed data for that purpose. Currently, the seismology community, through the Southern California Earthquake Center (SCEC) Broadband platform project (Goulet et al., 2015) is preparing their tools to produce physics-based synthetic data. The use of physics-based models (e.g. Dalguer et al, 2008; Olsen et al., 2009; Shi and Day, 2013; Baumann and Dalguer, 2014) appear to be the most suitable and reliable approach to generate ground motion in areas with lack of observations, because they provide meaningful extrapolations of strong ground motion prediction for future events. The SMART 2013 project (<http://www.smart2013.eu>), that has carried out a laboratory experiment on a shaking table under seismic loading to test a reduced scaled model (1/4 scale) of the half part of typical simplified electrical nuclear building of Reinforced Concrete (RC), has performed series of international benchmarks for the structural analysis of the mock-up, one of these benchmarks was for the evaluation of the vulnerability of the structure, in which our group has participated and reported in this paper. For that purpose, a database of 50 sets of synthetic accelerograms, each set composed by two horizontal components, is used. These synthetics are compatible with an earthquake of magnitude $M = 6.5$ at distance 9 km from the source. For now, these accelerograms are not physics-based synthetic, but they serve as an exercise to test our models. We are currently working in the

development of a database of physics-based synthetic ground motion for future calculations of fragility curves that will be reported elsewhere. The technical specifications of the SMART 2013 international benchmark that contains the general description of the benchmark and the mock-up, such as the seismic inputs, material parameters, recommendation for the structural analysis and calculation of fragility curves can be found in Richard and Chaudat (2014). The software ABAQUS (2013) was used for the nonlinear structural analysis. The geometry of the mock-up is a trapezoidal, three-story reinforced concrete structure. A picture, a plan view and the Finite Element (FE) Model of the structure are shown in Figure 1.

Figure 1. Mock-up structure: (a) 3D photo, (b) plan view showing position of the mock-up on the shaking table, actuator of seismic excitation, axis system of reference and points (A, B, C and D) of sensors where motions are recorded; (c) FE model



SMART project use a RC structure, because this type of structures are widely used in building structures, particularly in heavy structures such as those in nuclear power plants (NPPs). All structural elements of the mock-up were included in the model with the geometry and material characteristics provided by the benchmark project organizers (Richard and Chaudat, 2014). The RC columns and beams were modelled by Timoshenko (shear flexible) 3D beam element of type B31 with linear interpolation. All RC walls, slabs and the foundation beam were modelled with triangular (type S3R) and quadrilateral (type S4R) conventional large-strain shell elements. Walls and slabs contain rebars that are introduced in the FE model through the ABAQUS module that allows defining rebar layers for shell elements. The shaking table is assumed as semi-rigid shell. The 3D FE model (Figure 1c) is discretized with 3442 elements and 3078 nodes which results in 18468 degrees of freedom.

For the constitute model of concrete, there are several models proposed in the literature (e.g. Kaar et al., 1978; Lee and Fenves, 1998; Lubliner et al., 1989). Here, the concrete damage plasticity (CDP) model available in ABAQUS is used as constitutive model. The CDP is a modification of the Drucker–Prager plasticity model. For the purpose of our study, we set up in the CDP module of ABAQUS a simplified elastic perfectly-plastic. The reinforcement (steel) follows a bilinear-elastic perfectly-plastic model.

MODAL ANALYSIS: Calibration of the natural frequencies

For the purpose of setting our finite element model, we have first developed a modal analysis to calibrate our model in order fit the first natural frequencies observed in the lab. The total required number of modes was specified as 12. For extraction of the eigenvalues, Lanczos eigensolver and Rayleigh damping of 6% were used. Three different boundary conditions were considered: Case 1, the mock-up is fixed at the foundation level and is not loaded with additional masses; Case 2, the mock-up is fixed at the foundation level and is loaded with additional masses (as shown in Figure 1a, the mock-up was loaded with self-weight and additional loads). To simplify the numerical model, the additional masses were modelled as non-structural masses with mass proportional distribution on each slab. In Case 3, It is also

loaded with additional masses, but due to the simplification of the shaking table, distributed spring-dashpot elements that connect two points, one from the foundation beam and one from the shaking table, have been considered in the foundation to account for possible shaking table-structure interaction. These elements have been calibrated in order to fit the first two fundamental frequencies of the structure. The calibrated spring stiffness was $1.2 \cdot 10^4$ N/mm, $2.715 \cdot 10^3$ N/mm and $6 \cdot 10^6$ N/mm for directions X, Y and Z, respectively. The first three natural frequencies of the 3FE cases and the ones observed in the experiments are listed in Table 1. Case 3 results are consistent with the experiment. Figure 2 shows the first three mode shapes for the case 3. The three cases respond with complex vibration mode in the first and second mode, dominated by translational vibration in X and Y direction and a rotation of the structural system which originates from the unsymmetrical geometry configuration and stiffness difference of the mock-up. In the third mode shape the mock-up responds with torsional vibration mode.

Table 1: Natural frequencies [Hz] of experiment and the FE model

Mode	Experiment	Case 1	Case 2	Case 3
1	6.28	18.562	8.162	6.283
2	7.86	33.680	15.125	7.674
3	16.50	59.477	28.490	14.281

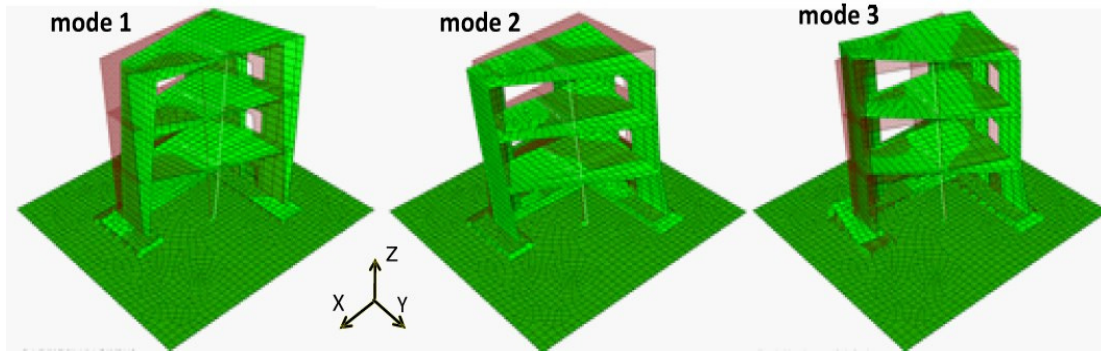


Figure 2. First three modes shape of FE model (case 3 with mock-up linked to the shaking table model through spring-dashpot elements)

LINEAR AND NONLINEAR DYNAMIC RESPONSE

We develop linear and nonlinear structural analysis using the implicit ABAQUS solver (using the Hilber-Hughes-Taylor time integration) under seismic excitation of the synthetic data mentioned before. The database of seismic excitation covers accelerograms with PGA values between 0.07g to 2.5g. For this analysis, distributed spring-dashpot elements have been used to represent the soil with stiffness and damping values given by the SMART project (Richard and Chaudat, 2014). Our results show that for weak seismic loading ($PGA < 0.3g$) the differences between linear and nonlinear solutions are minor. Nevertheless, for $PGA > 0.5g$ the differences are notable. As a typical example, Figure 3 shows the comparison of the floor-acceleration and -spectral acceleration at the top floor, of the structural response under the seismic excitation that has a PGA of 0.54g. As shown in Figure 3, the nonlinear material imposes limits to the accelerations of the structural response at frequencies around the first two fundamental frequencies of the structure, with amplitude reduction of about 50% of that of the linear response. The first two natural frequencies are excited in the response of the Y component, and the first frequency in the X component. Visible deviation from the linear response initiates at the beginning of the strong shaking. Drop of the first fundamental frequencies due to plastic damage is not observed in our calculations. Our conjecture is that this lack of frequency drop is attributed to the light damage experienced by the structure.

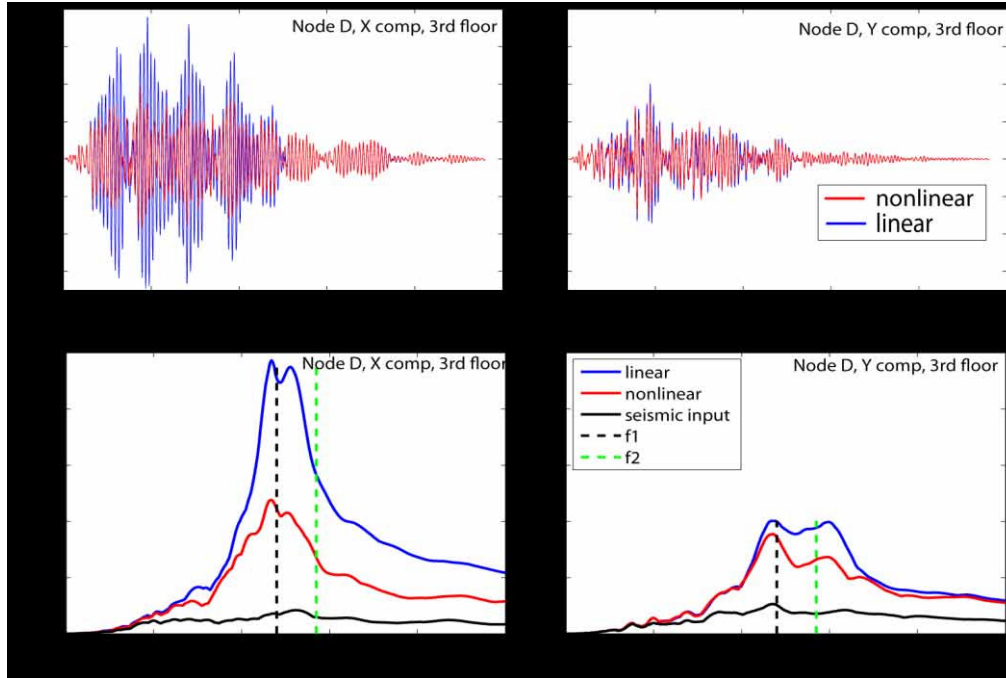


Figure 3. Comparison of the structural response, in point at top floor, under the seismic excitation with PGA of 0.54g calculated by linear and nonlinear analysis: (top) floor acceleration time history, (bottom) floor spectral acceleration. f1 (4.8 Hz) and f2 (5.7Hz) are, respectively, first and second fundamental frequency of the linear case.

FRAGILITY CURVES

A reliable assessment of seismic vulnerability of buildings depends mainly on the criteria to define the level of damage and threshold for failure criteria from the response of the structure under seismic excitation. This excitation is in turn characterized by seismic intensity or seismic indicator (hazard). Due to the intrinsic uncertainty (usually very large) in estimating the damage indicator, seismic indicator and structural response, the vulnerability analysis is performed in a probabilistic sense, that is, the conditional probability of obtaining a specific damage level for a given level of seismic indicator, the so called fragility curves. A thorough compilation of work on it is presented by (Calvi et al, 2006), in which they look at some of the most significant contributions in the field of vulnerability assessment. Here the recommendations of SMART project (Richard and Chaudat, 2014) for the calculation of fragility curves for both linear and nonlinear response of the structure were followed. Damage indicator is defined by the maximum inter-story drift at the top of the floor (in the X and Y directions). Three levels of damage are considered: Light damage (drift = $h/400$), controlled damage (drift= $h/200$), and extended damage (drift= $h/100$), where h is the story height. Three types of seismic intensity (seismic motion indicators) are used: The PGA, Cumulative Absolute Velocity (CAV) and the structure-specific Average Spectral Acceleration (ASA40) defined as the area obtained by integrating the response spectrum between 0.5 and 1 times the first fundamental frequency of the structure (De Biasio et al., 2014).

The fragility curve is commonly modeled by a lognormal cumulative distribution function, a choice supported by studies in the past in different fields (e.g. Ellingwood, 1990; Singhal and Kiremidjian, 1996; Shinozuka et al., 2000). Therefore, the fragility curve is mathematically described by

$$P_f(\theta) = \Phi\left(\frac{\ln(\theta/A_m)}{\beta}\right) \quad (1)$$

in which θ is, in our case, the seismic intensity or seismic motion indicators (PGA, CAV or ASA40), A_m is the median capacity expressed in units of θ , β is the lognormal standard deviation and Φ is the standard normal probability distribution function. The fragility curve (Equation 1) is then entirely determined by the two parameters, A_m and β . These two parameters can be determined by means of regression analysis or using maximum likelihood estimations (e.g. Kinali et al 2007, Shinozuka et al 2000, Zentner et al 2010, Zentner et al 2011). Here we perform a linear regression to predict maximum inter-story drift (D) at the top of the floor, for a given seismic indicator θ . The data used for this purpose are the drift obtained from the structural analysis under seismic excitation. The empirical relationship obtained by this analysis is a linear equation described by

$$\ln(D) = a + b \ln \theta \quad (2)$$

where a and b are coefficients obtained from the regression analysis. The median capacity is then calculated using Equation 2 assuming that the inter-story drift D reaches the critical threshold of damage indicator (D_d), that give the following expression:

$$\ln(A_m) = \frac{\ln(D_d) - a}{b} \quad (3)$$

The lognormal standard deviation β is computed from the dispersion of the data (obtained from the structural analysis) with respect to the Equation 2, that give the following expression:

$$\beta^2 = \frac{1}{N} \sum_{i=1}^N [\ln(D_i) - \ln(D)]^2 \quad (4)$$

where N is the number of data and D_i is the data i (from structural analysis)

Figures 4, 5 and 6 show, respectively, for the seismic indicators PGA, CAV and ASA40, the drift prediction (top figures) and the fragility curve (bottom figure). The results for the three seismic indicators follow in general similar features. The top figures are the natural logarithm of the drift vs PGA, for linear and nonlinear cases, with their corresponding line (predictor) calculated by linear regression. The predictor lines for linear and nonlinear cases are similar for the X direction, while for the Y direction the nonlinear case predicts larger values than the linear one. The bottom of each Figure (4,5 and 6) show the fragility curves for each seismic indicator. The prediction of the probability of damage substantially differs between the X and Y direction. More conservative prediction provides the linear analysis for the X direction, and the nonlinear case for the Y direction.

The lowest standard deviation is obtained for seismic indicator PGA and ASA40 (see Table 2), suggesting that these two parameters correlate better with the maximum drift. Therefore, for this case study, these seismic indicators are the best seismic characterization for the prediction of damage, assuming that the damage indicator defined here is appropriate. For the X direction the ASA40 is a better seismic indicator, but for the Y direction is the PGA. The standard deviation for the case with permanent drift is quite high.

Table 2: Lognormal standard deviation β for the linear and nonlinear calculations.

Seismic indicator	Linear (max. drift)		Nonlinear (max. drift)	
	X	Y	X	Y
PGA	0.28	0.23	0.23	0.28
CAV	0.37	0.36	0.33	0.35

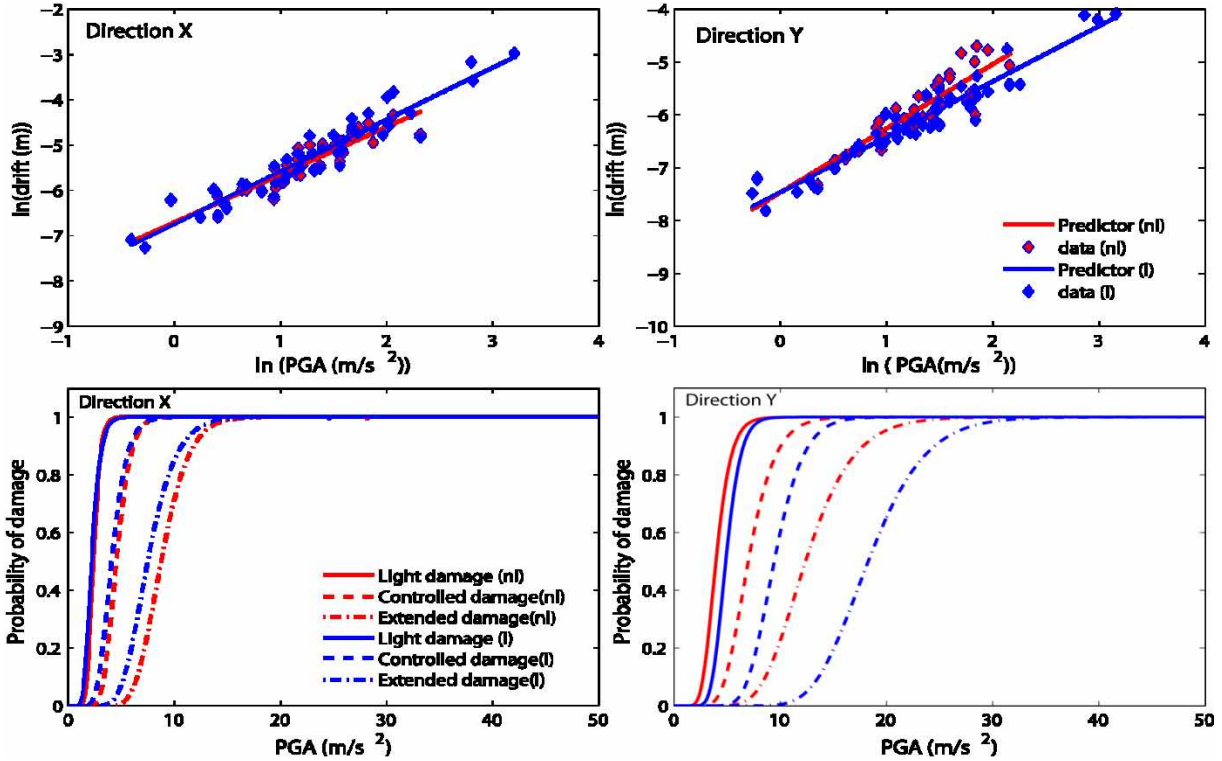


Figure 4. [Top] drift vs seismic indicator PGA. [bottom] Fragility curve for PGA, where *nlp*, *nl* and *l* in the legend are, respectively, nonlinear permanent drift, nonlinear and linear.

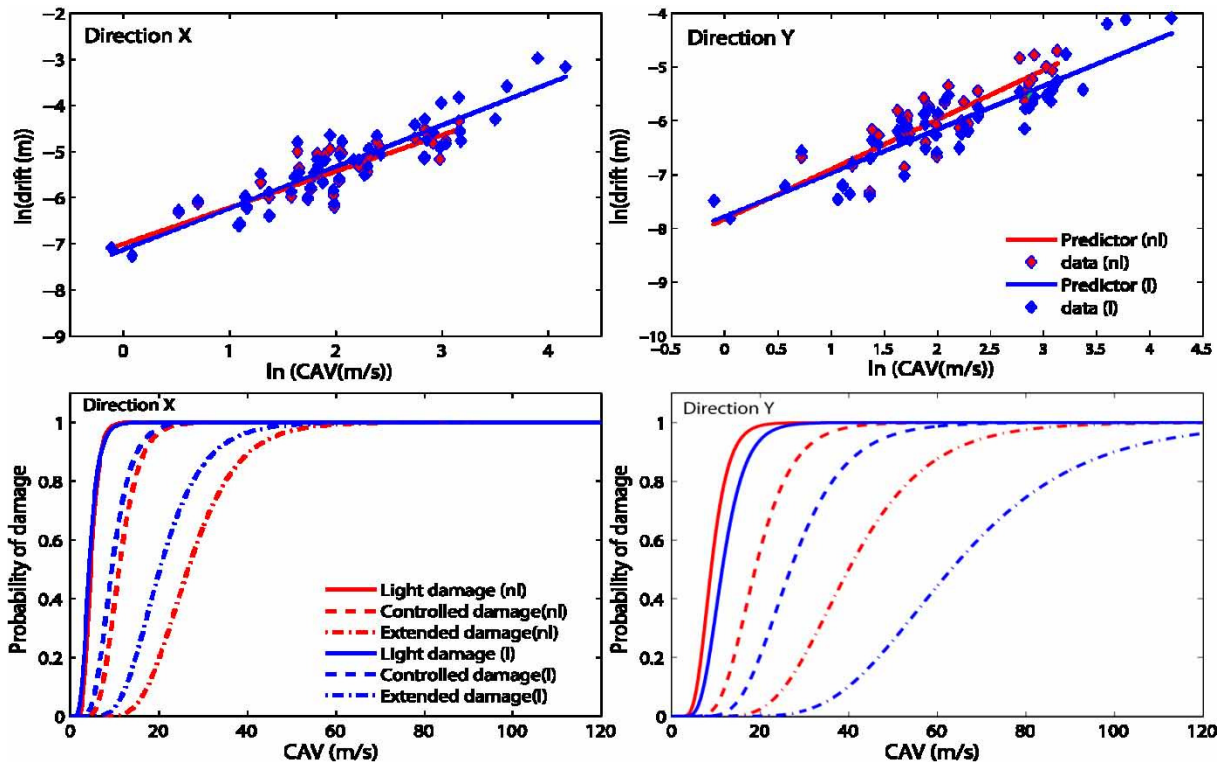


Figure 5. [Top] drift vs seismic indicator CAV. [bottom] Fragility curve for CAV, where *nlp*, *nl* and *l* in the legend are, respectively, nonlinear permanent drift, nonlinear and linear.

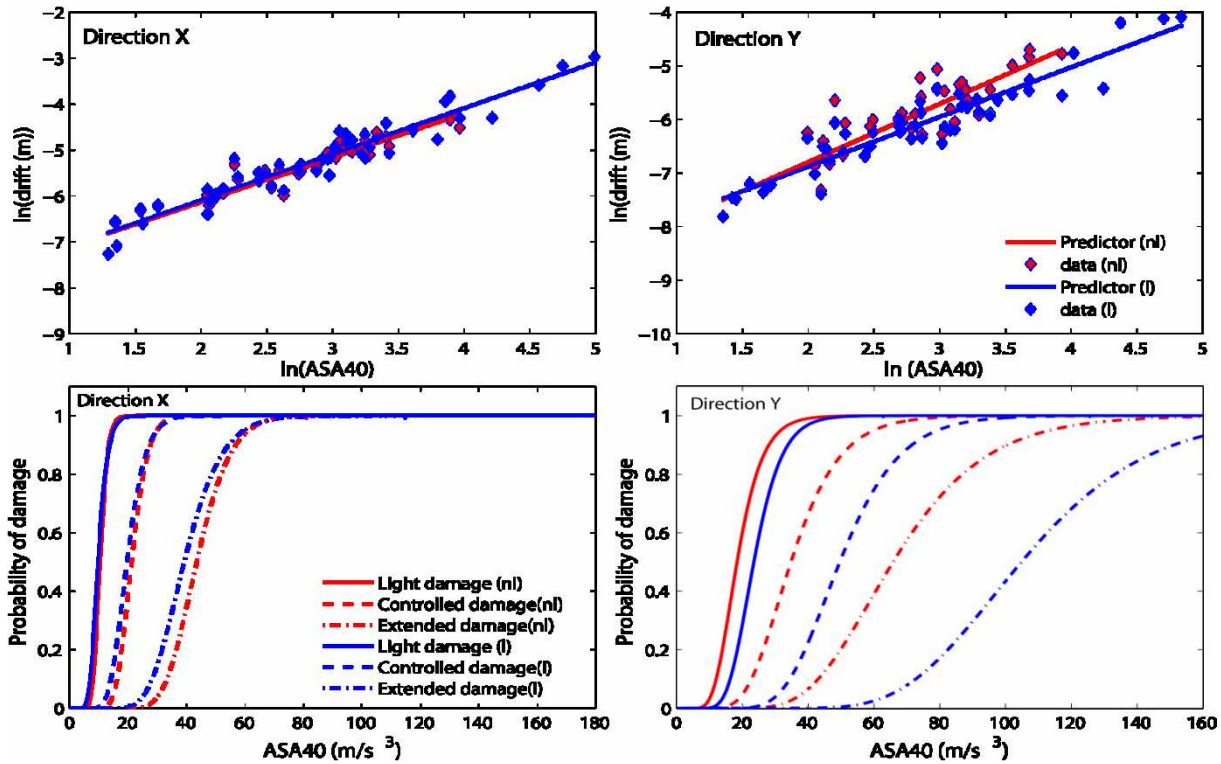


Figure 6. [Top] drift vs seismic indicator ASA40. [bottom] Fragility curve for ASA40, where *nlp*, *nl* and *l* in the legend are, respectively, nonlinear permanent drift, nonlinear and linear.

CONCLUSIONS

A 3D finite element model was developed, considering linear and material nonlinearity, using ABAQUS to evaluate fragility curves of a RC electrical nuclear structure of the SMART 2013 project under synthetic seismic excitation corresponding to a magnitude Mw 6.5 and a distance of 10 km from the source. Spring-dashpot elements have been introduced to represent the foundation that allows to fit the first two observed fundamental frequencies of the structure. The comparison between linear and nonlinear response of the structure shows that the nonlinear material imposes limits to the accelerations of the structural response at frequencies around the first two fundamental frequencies of the structure, with amplitude reduction of about 50% of that of the linear response. The largest inter-story drift occurs during the shaking, and visible deviation from the linear response initiates at the beginning of the strong shaking. Due to the unsymmetric characteristic of the structure, the prediction of the probability of damage substantially differs between the X and Y direction. More conservative prediction provides the linear analysis for the X direction, and the nonlinear case for the Y direction. For the case study in this paper and considering only the three seismic indicator used here, the seismic indicators PGA and ASA40 appear to be the best seismic characterization to predict maximum inter-story drift at the top of the structure. Therefore, within the assumptions that maximum drift is a good damage indicator, these two seismic indicators are good metrics to predict probability of damage.

We are aware that the assumption of elastic perfectly-plastic model for the concrete is too simplistic and unrealistic, because the mechanical properties of the concrete are actually expected to have strong nonlinearity since the beginning of loading. In this context, the conclusions of this paper have to be taken with caution and within the assumptions considered here. At present, we are developing a more exhaustive research with more realistic representation of the concrete that will be published elsewhere in the future.

It is also important to mention that at the last minute, we have realized that our finite element model has included reinforcement mainly in the vertical direction of the walls, and the amount of reinforcement in horizontal direction is quite low that is different to the real structure. The implications of this lack of reinforcements are going to be addressed during the SMiRT conference.

REFERENCES

- ABAQUS (2013). ABAQUS Inc. 2013, Version 6.13-1
- Baumann C. and L.A. Dalguer (2014). "Evaluating the Compatibility of Dynamic-Rupture-Based Synthetic Ground Motion with Empirical GMPE", *Bull. Seismol. Soc. Am.* 104(2), April 2014, doi: 10.1785/0120130077.
- Calvi G., Pinho R., Magenes G., Bommer J., Restrepo-Velez L. and Crowley H. (2006). "Development of seismic vulnerability assessment methodologies over the past 30 years", *Indian Society Journal of Earthquake Technology*, 43 (3), 75-104.
- Dalguer, L.A., H. Miyake, S.M. Day and K. Irikura (2008), "Surface Rupturing and Buried Dynamic Rupture Models Calibrated with Statistical Observations of Past Earthquakes". *Bull. Seismol. Soc. Am.* 98, 1147-1161, doi: 10.1785/0120070134.
- De Biasio M., Grange S., Dufour F., Allain F., Petre-Lazar I., (2014). "A simple and efficient intensity measure accounting for non-linear behavior of structures". (Submitted to Earthquake Spectra for publication).
- Ellingwood, B. (1990). "Validation studies of seismic PRAs", *Nuclear Engineering and Design*, 123(2): 189-196.
- Goulet, C.A., Abrahamson, N.A., Somerville, P.G. and K. E. Wooddell (2015). "The SCEC Broadband Platform Validation Exercise: Methodology for Code Validation in the Context of Seismic-Hazard Analyses", *Seismol. Res. Lett.*, 86, no. 1, doi: 10.1785/0220140104.
- Kaar, P.H., Hanson, N. W. and Capell, H.T. (1978). "Stress-strain curves and stress block coefficients for high strength concrete", *ACI Special Publication*
- Kinali K., Ellingwood B.R. (2007). "Seismic fragility assessment of steel frames for consequence based engineering: A case study for Memphis TN.", *Eng. Structures*, 29:1115-1127.
- Lee, J., Fenves G.L (1998). "Plastic-damage model for cyclic loading of concrete structures", *J. Engineering Mechanics*, 124 (10), 892-900.
- Lubliner, J., Oliver J., Oller S. and Onate E. (1989). "A plastic-damage model for concrete", *International Journal of Solids and Structures*, 25, 299-329.
- Olsen, K., S.M. Day, L.A. Dalguer, J. Mayhew, Y. Cui, J. Zhu, V.M. Cruz-Atienza, D. Roten, P. Maechling, T.H. Jordan, D. Okaya and A. Chourasia (2009). " ShakeOut-D: Ground motion estimates using an ensemble of large earthquakes on the southern San Andreas fault with spontaneous rupture propagation", *Geophys. Res. Lett.*, 36, L04303, doi:10.1029/2008GL036832.
- Richard B. and Chaudat T. (2014). "Presentation of the SMART 2013 International Benchmark", *Specification technique DEN, CEA, DEN/DANS/DM2S/SEMT/EMSI/ST/12-017/G.*
- Shi, Z., and S. M. Day (2013). "Rupture dynamics and ground motion from 3-D rough-fault simulations", *J. Geophys. Res.* 118, 1–20, doi: 10.1002/jgrb.50094.
- Shinozuka M., Feng, Q., Lee, J., Naganuma T. (2000). "Statistical analysis of fragility curves". *J. Eng. Mech. ASCE*, 126 (12), 1224-1231.

- Singhal, A. and Kiremidjian A.S. (1996). "Method for probabilistic evaluation of seismic structural damage", *Journal of Structural Engineering (ASCE)*, 122(12): 1459-1467.
- Woessner, J., D. Giardini and the SHARE consortium (2012). "Seismic Hazard Estimates for the Euro-Mediterranean Region: A community-based probabilistic seismic hazard assessment", *Proceedings of the 15th World Conference of Earthquake Engineering*, Lisbon, Portugal, Paper Nr. 4337, 2012.
- Zentner I., Humbert N., Ravet, S. Viallet E., (2011). "Numerical methods for seismic fragility analysis of structures in nuclear industry: application to a reactor coolant system", *Georisk* 5(2):99-109.
- Zentner I. (2010). "Numerical computation of fragility curves for NPP equipment", *Nuclear Engineering and Design*, 240(6):1614–21.